Macromolecules

ARTICLE

pubs.acs.org/Macromolecules

Acid Degradable and Biocompatible Polymeric Nanoparticles for the Potential Codelivery of Therapeutic Agents

Hien T. T. Duong,[†] Christopher P. Marquis,[‡] Michael Whittaker,[†] Thomas P. Davis,*[,†] and Cyrille Boyer*[,†]

[†]Australian Centre for NanoMedicine (ACN), School of Chemical Engineering, The University of New South Wales, 2052 NSW, Sydney, Australia

[‡]School of Biotechnology and Biomolecular Sciences, The University of New South Wales, 2052 NSW, Sydney, Australia

Supporting Information

ABSTRACT:

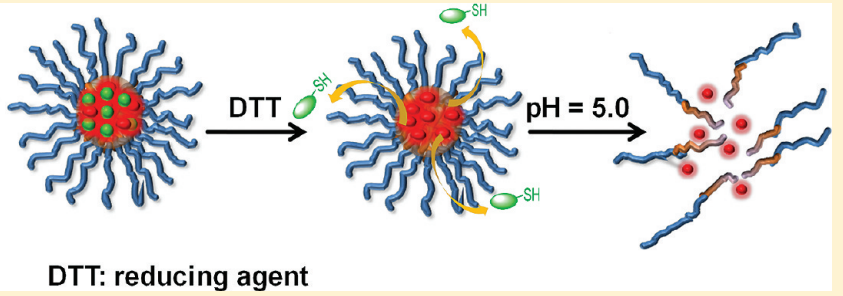

The synthesis of well-defined functional nanoparticles for the encapsulation of hydrophobic and hydrophilic drugs is described. Nanoparticles were built from amphiphilic copolymers consisting of P(OEG-A) homopolymers chain extended with vinyl benzyl chloride (VBC) and pentafluorophenyl acrylate (PFP-A) comonomers. Subsequently, the pendant chlorine atoms, introduced into the chains by VBC units, were substituted using sodium methanethiosulfonate, yielding copolymer chains with methanethiosulfonate (MTS) pendant functionality. The thiol/MTS exchange chemistry afforded by the MTS groups was then used to introduce different functional groups by reacting with a range of thiols. These copolymers were self-assembled in water yielding nanoparticles with sizes of ∼20 nm. The activated esters in the copolymer were used to cross-link the nanoparticles with difunctional amino compounds (cross-linkers). A cross-linker bearing an acid cleavable bond (ketal) was used to generate pH-sensitive core−shell nanoparticles. Drug encapsulation and release was modeled using hydrophobic (Nile Red) and hydrophilic (thiol-modified fluorescein isothiocyanate, FITC) dye molecules. The release of each dye was monitored using UV−vis spectroscopy, demonstrating the possibility of selective release of single dye or the simultaneous release of both dyes depending on the experimental stimuli. An *in vitro* study confirmed that the nanoparticles were nontoxic to the NIH-3T3 cell line. Cell uptake analysis by flow cytometry and fluorescence microscopy indicated a higher uptake for cross-linked nanoparticles than for non-cross-linked nanoparticles.

INTRODUCTION

Soft core−shell polymeric nanoparticles have been widely investigated as potential vectors for the sustained delivery of therapeutic payloads, such as drugs, proteins, genes, and imaging agents.[1−5] It is known that polymeric nanoparticles have prolonged circulation times in the bloodstream and allow effective accumulation in vascularized solid tumors due to the enhanced permeability and retention (EPR) effect.[6,7] The attraction of polymeric core−shell nanostructures as drug delivery platforms is further enhanced by the versatile modification chemistry available via the underlying copolymer functionality for multimodal applications.[8−10] Polymeric nanoparticles can be assembled from a range of polymer architectures, including dendrimers, micelles, star polymers, and vesicles, combs, brushes, and so on.[11−16] Diverse well-defined polymeric structures now can be obtained easily using living radical polymerization (LFR) approaches, e.g., atom transfer radical polymerization (ATRP)/metal mediated,[17−23] reversible addition−fragmentation transfer polymerization (RAFT),[24−32] and nitroxide-mediated polymerization (NMP).[33] In addition, the combination of LFR with click-chemistry techniques gives facile access to novel architectures in high yield.[34−37] Recently researchers have demonstrated the synthesis of core or shell cross-linked nanoparticles for the encapsulation of imaging agents, oligonucleotide, or drugs, exploiting different click reactions.[38−46]

To date, nanoparticles have been largely designed to encapsulate and deliver a single therapeutic agent. However, there is interest in designing multidelivery platforms, which are able to encapsulate

Received: May 12, 2011
Revised: August 14, 2011
Published: September 16, 2011

Scheme 1. Synthetic Scheme for Acid Degradable Amine Bearing Cross-Linker

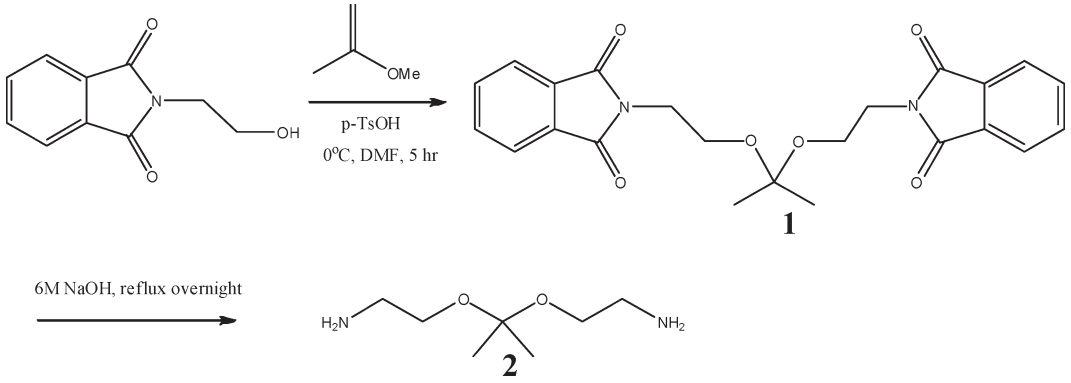

multiple payloads and to deliver them to targeted sites in a specific and controlled manner.[47] These multidelivery systems can exploit the synergic therapeutic effects of different drugs, offering promising new therapies. It has already been demonstrated that combining a chemotherapeutic agent with small interfering ribonucleic acid (siRNA)[48−51] or the combination of two different chemotherapeutic agents[52−56] in a single nanoparticle can significantly enhance the therapeutic effect of the individual compounds. Such multimodal systems have been proposed using multicompartment micelles obtained via self-assembled miktoarm star polymers[57−59] or ABC triblock copolymers,[60] where each compartment can be exploited to encapsulate a specific compound.[61,62] Despite these advances, strategies to precisely control the release rate of different therapeutic payloads from a single multidelivery platform are still limited.[63]

In this study, we describe the synthesis of new polymer nanoparticles which contain both methanethiosulfonate (MTS) and activated ester (pentafluorophenyl ester, PFP-A) pendant functionalities. These nanoparticles were assembled from predesigned block polymers synthesized via RAFT; the corona was formed from POEG-A (A-block) while the core domain (B-block) was composed of a random copolymer of vinyl benzyl chloride (VBC) and pentafluorophenyl acrylate (PFP-A). Both VBC and PFP-A have been previously successfully polymerized via RAFT or ATRP and subsequently modified, attaining very high yields, with a range of amino functional compounds giving nontoxic polymers.[34,64−71] By first reacting the VBC groups with sodium methanethiosulfonate, the orthogonal chemical attachment of model thiol and amine containing compounds in high yield is now possible. In this work a model hydrophilic payload, thiol-modified fluorescein isothiocyanate (FITC) was incorporated into the core via thiol−disulfide exchange reactions, while stabilization of the nanoparticles was subsequently achieved using a diamine cross-linker which contained a biodegradable acid cleavable bond (ketal). In addition, the hydrophobic cores of the nanoparticles were demonstrated to be suitable for carrying hydrophobic payloads (e.g., Nile Red) via nonspecific hydrophobic interactions.

The stable cross-linked nanoparticles degraded to unimers when subjected to mildly acidic conditions (pH = 5.0) (mimicking the endosomal/lysosomal environment of cells) while the release of FITC was stimulated by a reducing environment.

EXPERIMENTAL PART

Materials. Oligo(ethylene glycol) methyl ether acrylate (OEG-A), M_w = 480 g mol^{-1}, 99%, Sigma-Aldrich) and vinylbenzyl chloride (VBC) were deinhibited via a column of activated basic alumina. Deinhibited OEG-A and VBC were both stored at −18 °C. The initiator, 2,2′-azobis(isobutyronitrile) (AIBN), was crystallized twice from methanol. High-purity N_2 (Linde gases) was used for reaction solution purging. All the others chemical reactants were purchased from Sigma-Aldrich, supplied at the highest purity.

Characterization Methods. Characterization methods are reported in the Supporting Information.

Syntheses. *Synthesis of RAFT Agents.* The synthesis 3-(benzylsulfanylthiocarbonylsulfanyl)propionic acid (BSPA, Scheme 2) has been described in an earlier publication.[72] ^{1}H NMR (300 MHz, $CDCl_3$) δ (ppm from TMS): 2.85 (2H, t, J = 6.8 Hz, $CH_2C(O)OH$), 3.62 (2H, t, CH_2CH_2), 4.61 (2H, s, CH_2−Ph), 7.31 (5H, m, $CH(C_6H_5)$). ^{13}C NMR (75 MHz, $CDCl_3$) δ (ppm from TMS): 224.1, 179.2, 136.2, 130.7, 130.1, 129.2, 42.9, 34.4, 32.3.

Synthesis of Pentafluorophenyl Acrylate. The synthesis of pentafluorophenyl acrylate (PFP-A) has been described in a preceding publication.[72] ^{1}H and ^{19}F NMR spectra are given in Figure S1 of the Supporting Information. ^{1}H NMR (300 MHz, $CDCl_3$) δ (ppm from TMS): 6.1 (1H, dd, CH_2=), 6.3 (1H, m, CH_2=), 6.6 (1H, dd, CH_2=). ^{13}C NMR (75 MHz, $CDCl_3$) δ (ppm from TMS): 164.1, 142.2, 140.2, 134.7, 127.2. ^{19}F NMR ($CDCl_3$) δ (ppm): 152.7, 158.2, 162.5.

Synthesis of Thiol-Modified Fluorescein Isothiocyanate, FITC. Thiol-modified FITC was prepared according to the reported procedure.[8] Briefly, a mixture of FITC (20 mg, 0.052 mmol), cystamine dihydrochloride (6 mg, 0.026 mmol), and triethylamine (26 mg, 0.26 mmol) was dissolved in DMSO (1 mL) and stirred for 4 h. Tris(2-carboxyethyl)phosphine hydrochloride (17.6 mg, 0.062 mmol) was then added, and this reaction mixture was stirred for 1 h. The product was precipitated in ethyl ether and washed with water. The crude product was directly used for conjugation with the prepared nanoparticles.

*Synthesis of Acid Degradable Amine Bearing Cross-Linker (Compound **2**, Scheme 1).* Compound **1** was prepared according to known procedure with some minor modifications.[73] *N*-(2-Hydroxyethyl)phthalimide (15 g, 78.5 mmol, 1 equiv) was completely dissolved in dry *N*,*N*-dimethylformamide (DMF) (200 mL), and *p*-toluenesulfonic acid (150 mg, 0.78 mmol) was added. The solution was cooled in an ice bath, and 2-methoxypropene (7.52 mL, 78.5 mmol, 1 equiv) was added carefully to the solution. After 10 min of stirring, molecular sieve (5 Å) (100 g) was added. The reaction mixture was then stirred for 5 h at room temperature. Finally, the reaction mixture was quenched by the addition of triethylamine (TEA) (20 mL). To facilitate further purification, acetic anhydride (4 mL) was added to convert any unreacted alcohol groups into the corresponding acetate, and the reaction mixture was stirred overnight. The molecular sieves were removed by filtration. DMF was then removed under reduced pressure. The product that was precipitated during the solvents removal process was collected and recrystallized twice from ethyl acetate, yielding a white solid. Yield: 75%.

Scheme 2. Synthesis and Functionalization of pH-Sensitive Core−Shell Nanoparticles

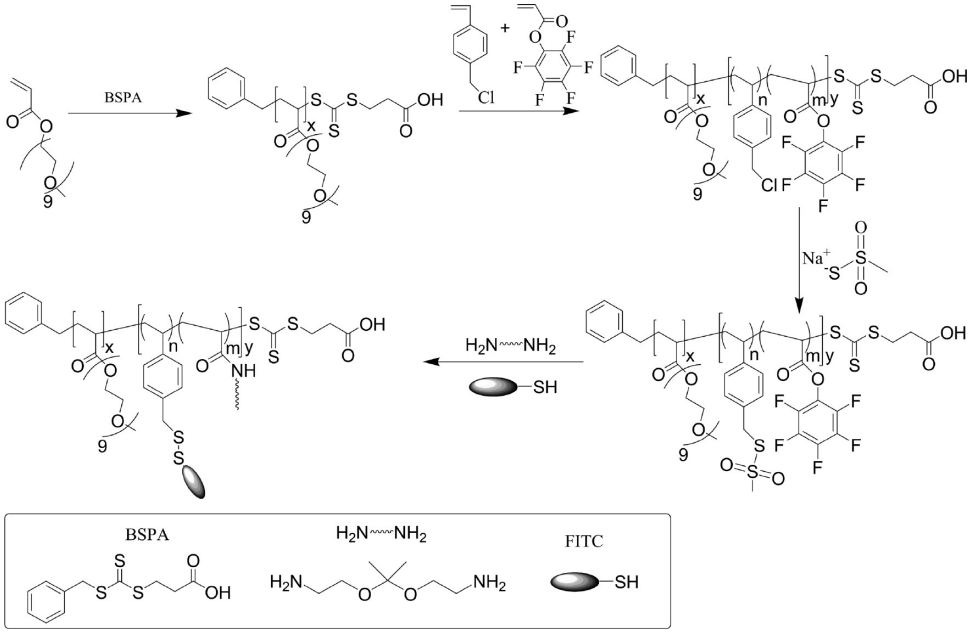

^{1}H NMR characterization was in accord with previous published data (Figure S2 in the Supporting Information).[74] ^{1}H NMR (300 MHz, $CDCl_3$) δ (ppm from TMS): 1.3 (6H, s, CH_3-C), 3.6 (4H, t, CH_2-O), 3.80 (4H, t, CH_2N), 7.4−7.8 (10H, dt, C_6H_5). ^{13}C NMR (75 MHz, $CDCl_3$) δ (ppm from TMS): 170.1, 132.2, 123.2, 113.7, 58.0.1, 42.9, 26.5.

Compound **1** was then deprotected using 6 M NaOH according to procedure in the literature, yielding the amber-color oil (compound **2**). Yield: 50%. ^{1}H NMR spectroscopy (Figure S3 in the Supporting Information) characterization was in good agreement with previous reported data.[74] ^{1}H NMR (300 MHz, $CDCl_3$) δ (ppm from TMS): 1.3 (6H, s, CH_3-C), 2.8 (4H, t, CH_2-NH_2), 3.60 (4H, t, CH_2O). ^{13}C NMR (75 MHz, $CDCl_3$) δ (ppm from TMS): 113.7, 64.2, 42.9, 26.5.

Synthesis of Homopolymer: Poly(oligoethylene glycol acrylate) (P(OEG-A)). Briefly, OEG-A_{480} (4.80 g, 1.0×10^{-2} mol), BSPA (77.0 mg, 2.86×10^{-4} mol), and AIBN (9.4 mg, 5.7×10^{-5} mol) were dissolved in acetonitrile (20 mL) in a round-bottom flask equipped with a magnetic stirrer bar. The flask was then sealed with a rubber septum and purged with nitrogen for 30 min in an ice bath. The reaction mixtures were then immersed in a preheated oil bath at 65 °C. After 5 h, the polymerization was terminated by placing the samples in an ice bath for 5 min. Acetonitrile was removed under reduced pressure, and the concentrated reaction mixture was purified by dialysis against methanol to remove any traces of monomer and unreacted reactants using a membrane cutoff (3500 Da). The solvent was evaporated, and the polymer product was analyzed by GPC and by NMR. Monomer conversion was calculated according the following equation: $\alpha^M = \int I^{CH=CH_2 5.5-6.5\ ppm} / \int I^{OCH_3 3.3\ ppm}$. After 5 h, a conversion of 58% was obtained. The molecular weight of the P(OEG-A) macro-RAFT agent was measured to be 10 200 g mol^{-1} (PDI = 1.14) by DMAc GPC, in good agreement with $M_{n(theo)}$ = 10 000 g mol^{-1}. M_n determined by NMR is also in good agreement with M_n(GPC).

Synthesis of Poly(oligo(ethylene glycol) methyl ether acrylate)-block-poly(vinylbenzyl chloride-co-pentafluorophenyl acrylate) (P(OEG-A)-b-P(VBC-co-PFP-A)). P(OEG-A)-*b*-P(VBC-*co*-PFP-A) was prepared by the chain extension of P(OEG-A) ($M_{n(theo)}$ = 10 000 g mol^{-1}, $M_{n(GPC)}$ = 10 200 g mol^{-1}) using vinylbenzyl chloride (VBC) and pentafluorophenyl acrylate (PFP-A) as comonomers. The number of repeating units (20) of OEG-A and PFP-A was calculated from the monomer conversion obtained from ^{1}H NMR and ^{19}F NMR, respectively (see for PFP-A, Figure S4 in the Supporting Information).

The P(OEG-A) macroRAFT agent (1 g, 1.00×10^{-4} mol), VBC (0.325 g, 2.11×10^{-3} mol), and PFP-A (0.175 g, 7.30×10^{-4} mol) were dissolved in acetonitrile (5 mL) in a round-bottom flask. The reaction mixture was purged with nitrogen for 30 min, and polymerization was carried out in a preheated oil bath at 65 °C for 14 h. The polymerizations were halted by cooling (an ice bath for 5 min). After 14 h polymerization, conversions of 80% for VBC and 70% for PFP-A (using signal at 6.0 ppm) were determined by ^{1}H NMR analysis, corresponding to 17 and 12 repeating units of VBC and PFP-A, respectively. The molecular weight of the P(OEG-A_{20})-*b*-P(VBC_{17}-*co*-PFP-A_{12}) was measured to be 15 500 g mol^{-1} (PDI = 1.35) by DMAc GPC, in good agreement with $M_{n(theo)}$ = 16 000 g mol^{-1}. The copolymer was purified by dialysis against acetone using membrane cutoff (6000−8000 Da) for 2 days to remove unreacted VBC and PFP-A (confirmed by ^{1}H and ^{19}F NMR analysis). Acetone was then removed under reduced pressure, and the purified copolymer was kept at 2 °C prior to further experiments.

Chemical Modification of Copolymers P(OEG-A_{20})-b-P(VBC_{17}-co-PFP-A_{12}) Using Sodium Methanethiosulfonate. The pendant chlorine atoms introduced to the polymer chains by VBC units were substituted using sodium methanethiosulfonate, yielding copolymer chains with MTS pendant groups. P(OEG-A_{20})-*b*-P(VBC_{17}-*co*-PFP-A_{12}) copolymer (1.5 g, 1×10^{-4} mol) and sodium methanethiosulfonate (0.34 g, 2.5×10^{-3} mol) were dissolved in dimethylformamide (DMF, 10 mL). The solution was then stirred overnight at room temperature, and the modified polymer was dialyzed against methanol to remove unreacted sodium methanethiosulfonate for 1 day at 20 °C. Methanol was removed under reduced pressure, and the copolymer was kept at 2 °C prior to further use. The copolymers were analyzed using ^{1}H NMR, ^{19}F NMR using $CDCl_3$ as solvent, and GPC.

Self-Assembly of P(OEG-A_{20})-b-P(VBC_{17}-co-PFP-A_{12}) Copolymer into Micellar Structure. Copolymer P(OEG-A_{20})-*b*-P(VBC_{17}-*co*-PFP-A_{12}) (40 mg) was dissolved in DMF (2 mL), which is a good solvent for both hydrophobic

and hydrophilic blocks. Distilled water (8 mL) was added dropwise (one drop per 10 s) to 2 mL of copolymer solution in DMF (20 mg mL^{-1}) under moderate stirring at room temperature. The mixture was then dialyzed against water for 2 days using membrane cutoff (3500 Da) to remove DMF. The targeted final polymer concentration was 4 mg mL^{-1}.

Synthesis of Core Cross-Linked Nanoparticles. Typically, a polymer solution (4 mg mL^{-1}) (5 mL) in distilled water was used for the core cross-linking reaction. Acid-degradable amine-bearing cross-linker (**2**) (0.005 g, 2.9×10^{-5} mol) was added, and the mixture was stirred overnight. The core cross-linked polymer was purified using membrane dialysis (molecular weight cut off of 3500 Da) for 2 days against distilled water to remove the unreacted cross-linker (confirmed by ^{1}H NMR). The yield of the reaction was calculated by freeze-drying a small amount of the crude product and analyzed by ^{19}F NMR analysis (Figure S5 in the Supporting Information). This measurement was also confirmed by using the following method.

Determination of Cross-Linking Density. ^{19}F NMR was used to determine the cross-linking density, exploiting trifluoroacetic acid (TFA) as an internal standard to determine the decrease of activated pentafluorophenol ester signal (at −152, −158, and −163 ppm) during the cross-linking process. The percentage of cross-linking was calculated by comparing the integral of the copolymer ^{19}F NMR signals before and after the reaction of acid sensitive cross-linker; see Supporting Information for details.

Encapsulation and Release of Thiol-Modified FITC and Nile Red. Thiol-modified FITC was synthesized according to a known procedure.[9] Thiol-modified FITC was reacted with pendant MTS groups to yield a disulfide linkage and release of methyl sulfonate (sulfinic acid) as leaving group. To generate the nanoparticles loaded with thiol-modified FITC, copolymer (20 mg, 1.33×10^{-6} mol) was dissolved in DMF (1 mL) in the presence of thiol-modified FITC (4.4 mg, 9.0×10^{-6} mol). The reaction was performed overnight at room temperature. The copolymer loaded with modified FITC was then self-assembled into micelles by the slow addition of water. Cross-linker **2** was added to stabilize the nanoparticles. The nanoparticles were purified by dialysis against water to remove unreacted reactants.

Subsequently, the loading of hydrophobic Nile Red to the nanoparticles was carried out. Typically, copolymer (20 mg, 1.33×10^{-6} mol) and Nile Red (2 mg) were dissolved in DMF (1 mL). Water was then added to this solution forming nanoparticles. Cross-linker **2** was used to stabilize the nanoparticles. Excess insoluble Nile Red was removed by filtration. The nanoparticles were purified by dialysis against water to remove DMF and unreacted cross-linker.

To investigate the duel loading/release, both thiol-modified FITC and Nile Red were loaded into the nanoparticles utilizing the similar procedure reported for the loading of single dye. Nile Red (10 wt % of polymer) was added to the solution of copolymer, which was modified with thiol-modified FITC, followed by dropwise addition of distilled water (5 mL). The dye-encapsulated nanoparticles were then stabilized by core cross-linking using cross-linker (compound **2** in Scheme 1) according to the procedure described above.

The nanoparticles loaded with thiol-modified FITC and Nile Red were subjected to reducing agent and/or to mildly acidic conditions (pH = 5). The cross-linked nanoparticle solution was equally divided into three samples. DL-Dithiothreitol (DTT) was added to the first sample (DTT in the polymer solution was 20 mM). The second sample was subjected to acidic conditions by the addition of HCl solution (0.5 mol L^{-1}) adjusting the pH of the medium to 5.0. The last samples were incubated in the presence of DTT (20 mM) and at a pH 5.0. All samples were incubated at 37 °C for 24 h. The release of guest molecules was monitored using UV−vis spectroscopy.

Cell Study. *Cell Culture.* NIH-3T3 cells were cultured in growth media consisting of Dulbecco's Modified Eagle's Medium: Nutrient Mix F-12 (DMEM) supplemented with 10% (v/v) Fetal Bovine Serum (FBS) in a ventilated tissue culture flask T-75 and passaged every 2−3 days when monolayers at around 80% confluence. The cells were used only when stable cell growth was obtained (approximately 3−4 passages). The cells were incubated at 37 °C in a 5% CO_2 humidified atmosphere. The cell density was determined by counting the number of viable cells using a trypan blue dye (Sigma-Aldrich) exclusion test. The cells were detached using 0.05% trypsin-EDTA (Invitrogen), stained using trypan blue dye, and loaded on the hemocytometer. One day prior to the treatment, the cells were seeded at required cell densities on tissue-culture-treated 24-well and 96-well plates. The un-cross-linked and cross-linked nanoparticles were labeled with thiol-modified FITC for the cell study. All the cell experiments were done in triplicate.

Cell Viability. The un-cross-linked and cross-linked nanoparticles were labeled with thiol-modified FITC. The cytotoxicity of fluorescein-labeled un-cross-linked and cross-linked nanoparticles was tested *in vitro* by a standard CellTiter-Blue Cell Viability Assay (Promega), which provides a homogeneous, fluorescent method for monitoring cell viability. The assay is based on the ability of living cells to convert a redox dye (resazurin) into a fluorescent end product (resorufin). Nonviable cells rapidly lose metabolic capacity and thus do not generate a fluorescent signal. The cells were seeded in a tissue culture treated 96-well plate in 100 μL medium per well at a density of 1000 cells/well and incubated for 24 h. The medium was then replaced with fresh medium containing un-cross-linked and cross-linked nanoparticles and incubated for 48 h. The final concentration of polymer in the wells was adjusted to desired concentrations ranging from 0.01 to 15 mg mL^{-1} in DMEM media containing 10% v/v FBS. CellTiter-Blue assay dye (20 μL) was then added to each well, and the cells were then incubated for 2 h. After an incubation step, data were recorded using a fluorescence plate reader (579ex/584em).

The amount of fluorescence produced (F) was proportional to the number of metabolically active (viable) cells in the culture. Wells without cells was set up as the negative control for the determination of background fluorescence. Wells without treatment with nanoparticles was used as the positive control. The cell viability was calculated by comparing the fluorescence products of treated and nontreated cells according to eq 1:

$$\text{cell viability } (\%) = \left(\frac{\overline{F}_{\text{sample}} - \overline{F}_{\text{negative control}}}{\overline{F}_{\text{positive control}} - \overline{F}_{\text{negative control}}} \right) \times 100\% \quad (1)$$

where $\overline{F}_{\text{sample}}$, $\overline{F}_{\text{negative control}}$, and $\overline{F}_{\text{positive control}}$ are the average fluorescence product in the sample wells (cell treated with polymeric nanoparticles), the average fluorescence product in the negative control wells (without cells), and the average fluorescence product in the positive control wells (without nanoparticles).

In Vitro Cell Uptake by Flow Cytometry and Fluorescence Microscopy. NIH-3T3 cells were seeded at a density of 1×10^5 cells/well in 24-well plates. The cells were left to grow for 24 h in DMEM media containing 10% FBS at 37 °C in 5% CO_2 atmosphere. On the next day, un-cross-linked and cross-linked nanoparticles dissolved in PBS were added into the wells (total volume 1 mL DMEM media containing 1% v/v PBS). The final concentration of polymer in the wells was adjusted to 0.05 mg mL^{-1} in DMEM media containing 1% v/v PBS.

Flow Cytometry. NIH-3T3 cells grown in 24-well plates were treated as described above. After 2 days incubation, cells were prepared for flow cytometry measurement. Briefly, cells were harvested by trypsinization and washed twice in PBS plus 0.5% BSA. The cells were then resuspended in PBS plus 0.5% BSA and filtered via the cell strainer having pore size of 40 μM prior to analysis by a Cell Lab Quanta SC flow cytometer (Beckman Coulter) in 10 000 cells. NIH-3T3 cells that were not treated with polymer solution were used as a control. Fluorescence concentration (FC), which represents the normalization

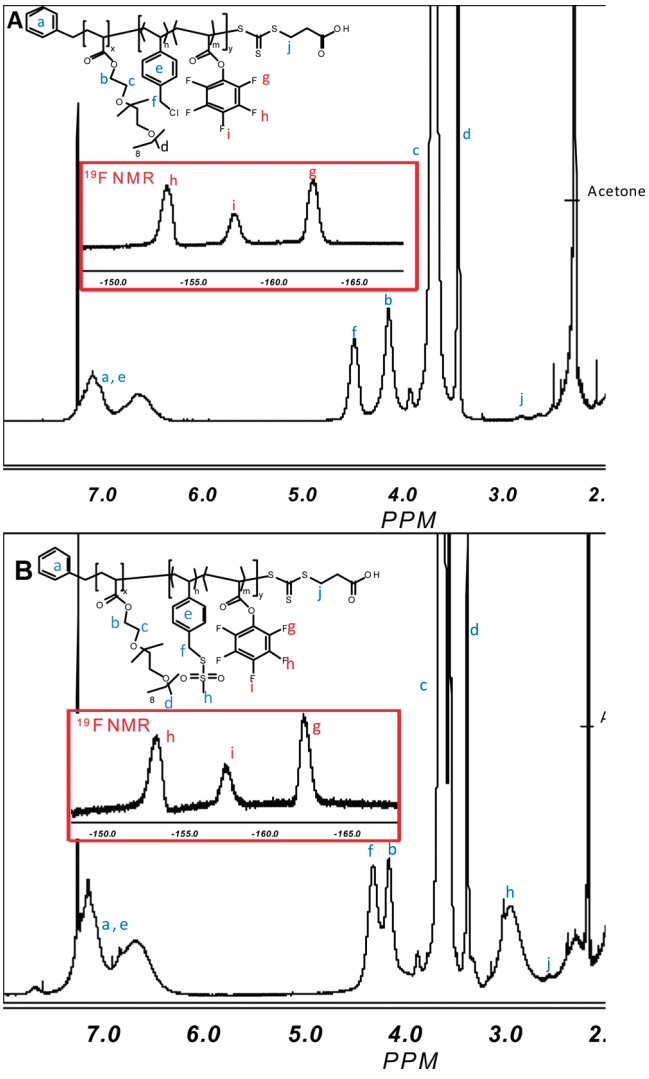

Figure 1. ^{1}H NMR spectra of P(OEG-A)-*b*-P(VBC-*co*-PFP-A) copolymers before (A) and after modification (B) with sodium methanethiosulfonate. ^{19}F NMR spectra are given in the inset.

of cell size or volume with fluorescent intensity, was used to evaluate cell uptake of prepared polymers. FC can be easily calculated using the instrument software. FC is calculated by dividing the fluorescence intensity value of the stained cells divided by the mean cell volume (eq 2).

$$\mathrm{FC} = \frac{\text{fluorescence channel}}{\text{volume channel}} \quad (2)$$

Fluorescence Microscopy. NIH-3T3 cells were treated with different samples in a 5 mm diameter glass coverslip (Deckglaser) inside the 24-well plate. Prior to the cell seeding, the glass coverslips were sterilized using 95% ethanol for 4−6 h. After 2 days of incubation, the coverslips were then taken out and rinsed with PBS twice to ensure that samples that were not taken up by cells were completely removed. Fluorescence expression in cells was observed after 2 days using an Olympus BX61 fluorescence microscope and DP-BSW image capture and control software with equal exposure time.

RESULTS AND DISCUSSION

Synthesis of Amphiphilic P(OEG-A$_{20}$)-*b*-P(VBC$_{17}$-*co*-PFP-A$_{12}$) Copolymer via RAFT Polymerization and Its Chemical Modification with Sodium Methanethiosulfonate. The amphiphilic functional block copolymers were synthesized via RAFT polymerization. Poly(oligoethylene glycol acrylate) homopolymer A-block (P(OEG-A)) was first synthesized using 3-(benzylsulfanylthiocarbonylsulfanyl)propionic acid (BSPA, Scheme 2) as the chain transfer agent and AIBN as an initiator, at 65 °C for 5 h. The polymerization was quenched at low monomer conversion (50−60%) to maintain high end-group functionality, and monomer conversion was determined via ^{1}H NMR analysis using the following equation: $\alpha^{\mathrm{OEG\text{-}A}} = [\int I^{\mathrm{CH{=}CH_2\ 5.5-6.5\ ppm}} / \int I^{\mathrm{OCH_3\ 3.6\ ppm}}] \times 100$, where $\int I^{\mathrm{CH{=}CH_2\ 5.5-6.5\ ppm}}$ and $\int I^{\mathrm{OCH_3\ 3.3\ ppm}}$ correspond to intensities from acrylate bond of OEG-A and methyl ether. After purification of the homopolymer by dialysis, P(OEG-A) was analyzed by GPC and ^{1}H NMR. ^{1}H NMR analysis reveals the characteristic signals of OEG-A at 4.0, 3.6, 3.3, and 1.5−2.0 ppm attributed to CH_2O ester, CH_2O ether, CH_3O, and $CH-CH_2$ backbone, respectively (Figure S6 in the Supporting Information). The presence of the RAFT end-group was confirmed by UV−vis spectroscopy (absorbance peak centered at 305 nm, data not shown) and by ^{1}H NMR analysis, with resonances visible at 7.2−7.3 ppm (benzyl group) and at 2.8 ppm ($S-CH_2$ signal). The conservation of the RAFT end-group was found to be over 95%, calculated via the equation $f^{\mathrm{RAFT}} = \int I^{\mathrm{CH_2\ 2.8\ ppm}} / \int I^{\mathrm{CH\ 7.2\ ppm}} \times 100$.

The number-average molecular weights (M_n) determined by GPC and NMR analysis (according to the equation $M_{n\ (\mathrm{NMR})} = (5 \times \int I^{\mathrm{CH_2O\ 4.0\ ppm}}/2 \times \int I^{\mathrm{CH\ 7.2\ ppm}}) \times \mathrm{MW}^{\mathrm{OEG\text{-}A} } + \mathrm{MW}^{\mathrm{BSPA}}$, where $\int I^{\mathrm{CH_3O\ 3.6\ ppm}}$, $\int I^{\mathrm{CH_2O\ 4.0\ ppm}}$, $\mathrm{MW}^{\mathrm{MA}}$, and $\mathrm{MW}^{\mathrm{BSPA}}$ correspond to intensities from OEG-A (methyl ester) and BSPA RAFT agent (benzyl group) and the molar mass of monomer and RAFT agent, respectively) are in good agreement. The P(OEG-A) macro-RAFT was then chain extended in the presence of pentafluorophenyl acrylate (PFP-A) and vinylbenzene chloride (VBC) comonomers at 65 °C for 14 h (Scheme 2). By adjusting the ratio of the two monomers, the number of functional groups in the copolymer B-block can be easily controlled. ^{1}H NMR analysis confirmed the presence of all signals associated with P(OEG-A) block and VBC block (Figure 1A) by the presence of typical signals at 6.8−7.5 and 4.5 ppm, associated with the signal from benzyl group and $-CH_2Cl$, respectively. ^{19}F NMR spectroscopy was used to confirm the presence of PFP-A units in the B-block (inset in Figure 1A). The composition of PFP-A in the copolymer was determined by using trifluoric acid (TFA) as an internal reference (calculation details are given in Supporting Information; see Figure S7). The monomer composition of PFP-A in the copolymer can be tuned by the initial feed ratio. P(OEG-A) ($M_{n(\mathrm{theo})}$ = 10 000 g mol^{-1}) was chain extended using three different concentrations of VBC ranging from 25 to 75 mol %, yielding three different P(OEG-A)-*b*-(VBC-*co*-PFP-A) copolymers. Table 1 shows the different copolymer compositions of VBC and PF-A. The composition in PFP-A in the final block copolymer is slightly lower than the initial feed ratio and is attributed to a difference of monomer reactivity.

The successful chain extension of P(OEG-A) was confirmed via GPC analysis by the shift in the GPC chromatogram from low molecular weight to higher molecular weight. The polydispersity index (PDI) remained rather low after chain extension (PDI ∼ 1.35) (Figure S8 in the Supporting Information). The VBC units in the B-block were postmodified using sodium methanethiosulfonate resulting in the introduction of reactive MTS groups.[75] ^{1}H NMR confirmed the quantitative substitution of the pendent chlorine group with the MTS moiety by the shift of signals from

Table 1. Copolymers Synthesized in This Study

			feed ratio (mol %)[b]		composition (mol %)[c]	
polymers	M_n (g mol^{-1})[a]	PDI[a]	PFP-A	VBC	PFP-A	VBC
P(OEG-A)-1	10 200	1.14				
P(OEG-A)-*b*- P(VBC-*co*-PFP-A)	15 500	1.35	75	25	65	35
P(OEG-A)-*b*- P(VBC-*co*-PFP-A)	15 200	1.32	50	50	45	55
P(OEG-A)-*b*- P(VBC-*co*-PFP-A)	14 900	1.33	25	75	20	80
P (OEG-A)-*b*- P(VBS-*co*-PFP-A)[d]	15 800	1.35				
P(OEG-A)-*b*- P(VBS-*co*-PFP-A)[d]	15 600	1.31				
P(OEG-A)-*b*-P(VBS-*co*-PFP-A)[d]	15 400	1.34				

[a] Assessed by DMAC GPC. [b] Initial feed ratio in mol %. [c] Assessed by ^{1}H NMR and ^{19}F NMR analyses (see Figure S9 in the Supporting Information). [d] P(OEG-A)-*b*-P(VBS-*co*-PFP-A) copolymers were prepared by postmodification via nucleophilic substitution of chloride atom by sodium methanethiosulfonate.

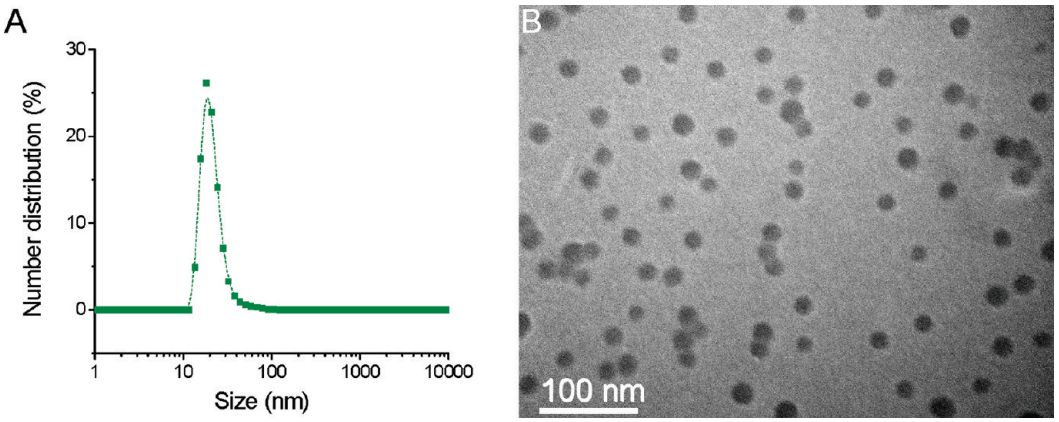

Figure 2. TEM and DLS analysis of self-assembled nanoparticles (polymer concentration of 1 mg mL^{-1} in water). OsO_4 vapor staining, scale bar = 100 nm.

4.5 ppm ($-CH_2-Cl$) to 4.2 ppm ($-CH_2-MTS$) and the appearance of new resonances at 3.3 ppm associated with the $-S-S(O)_2-CH_3$ group (Figure 1B). ^{19}F NMR spectroscopy confirms that PFP-A was not affected by the modification of VBC with MTS (Figure 1 inset and Figure S9 in the Supporting Information). However, it should be noted that the addition of a large excess of MTS compared to VBC can result in some side reactions involving the PFP-A comonomer, originating from nucleophilic aromatic substitution reactions of MTS at the para-position of the pentafluorophenyl functionalities. It is noteworthy that this modification did not alter the number-average molecular weight of the polymer as confirmed by GPC analysis (see Table 1).

Self-Assembly of the Copolymers in Aqueous Solution. The assembly of the amphiphilic block copolymers in aqueous media to form different morphologies has been intensively investigated by others.[76−79] Eisenberg and co-workers have done extensive research into factors that control the morphology of self-assembled copolymers such as absolute and relative block length, the water content of the solvent mixture, the nature and the presence of additives (ions, homopolymers, and surfactants), and the PDI of the block copolymers.[80] It is widely known that morphology of these self-assembled systems is influenced by the preparation method.[81,82] In this work, water was added slowly to the stirred copolymer/DMF solution to yield micelles. The self-assembly of copolymers in water was confirmed via DLS and TEM (Figure 2). The mean particle size of un-cross-linked nanoparticles in water, as derived from DLS data, was ca. 20 nm (by number-average), in good agreement with TEM micrographs. Volume and intensity distribution obtained by DLS are presented in the Figure S10 of the Supporting Information.

Synthesis of Biocompatible and pH-Sensitive Core Cross-Linked Nanoparticles. Self-assembled structures are dynamic, with a tendency to dissociate at very low concentrations.[83,84] This dissociation has been correlated with the length of the hydrophobic block, with a short core-forming block resulting in less stable aggregates, while longer block lengths result in more thermodynamically and kinetically stable structures.

The presence of activated ester (PFP-A) in the backbone of copolymer was exploited to cross-link the nanoparticles using a specifically designed difunctional amine compound; the acid-degradable amine bearing cross-linker **2** was prepared according to the procedure published by Frechet and co-workers[73] after yield optimization (the yield was increased from 50% to 75%). Following the self-assembly process, cross-linker **2** was introduced to react with the PFP-A group, and the cross-linking reaction was monitored by ^{19}F NMR. The cross-linking yield was calculated from ^{19}F NMR data by comparing the integrals of the copolymer signals at −152, −158, and −164 ppm before and after the reaction with the cross-linker. The cross-linking density was 75% (data not shown), which is sufficient to form a fully cross-linked network in the core. The excess pentafluorophenyl

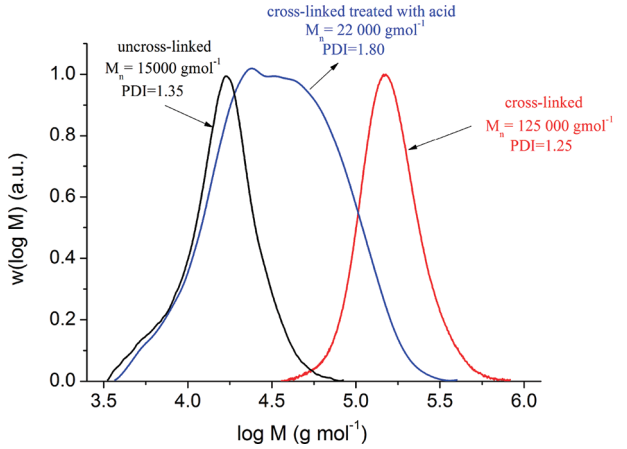

Figure 3. Comparison of GPC chromatograms of un-cross-linked (black line), cross-linked polymer (red line), and cross-linked polymer after treatment with acid (blue line).

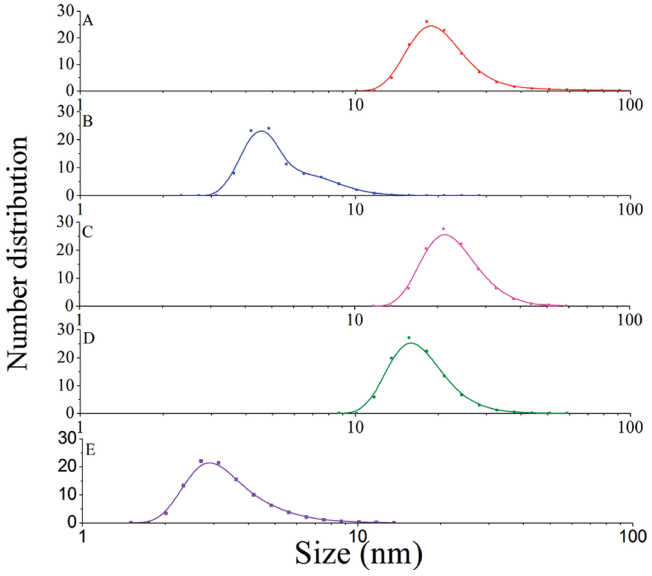

Figure 4. Hydrodynamic diameters assessed by DLS (concentration of copolymer of 1 mg mL^{-1}) of un-cross-linked and cross-linked nanoparticles (NP) before and after treatment with acid: A, un-cross-linked micelle in water; B, un-cross-linked micelle in DMAc; C, cross-linked micelle in DMAc; D, cross-linked in water; E, cross-linked after treatment with acid in DMAc.

groups in the polymer were removed using a low molecular weight hydrophobic amine (hexylamine) converting all the remaining pentafluorophenyl groups.

The cross-linked nanoparticles were characterized by DMAc GPC as DMAc is a good solvent for both blocks. These cross-linked nanoparticles can also be considered as nanogel centered "stars" which are still suitable for analysis by GPC.[82,85] A substantial shift in retention time (or molecular weight) from the block copolymers to the cross-linked structures was noted (15 000 to 125 000 g mol^{-1}), which confirmed a successful cross-linking reaction. The cross-linked sample (PDI = 1.25) showed only one narrow peak on the GPC chromatogram, indicating the absence of free unimers (Figure 3). It should be noted that the molecular weight assessed by GPC is not absolute because of the use of linear polystyrene standards for GPC

Scheme 3. Schematic Representation for the Loading of (A) FITC, (B) Nile Red, and (C) and Both Dyes

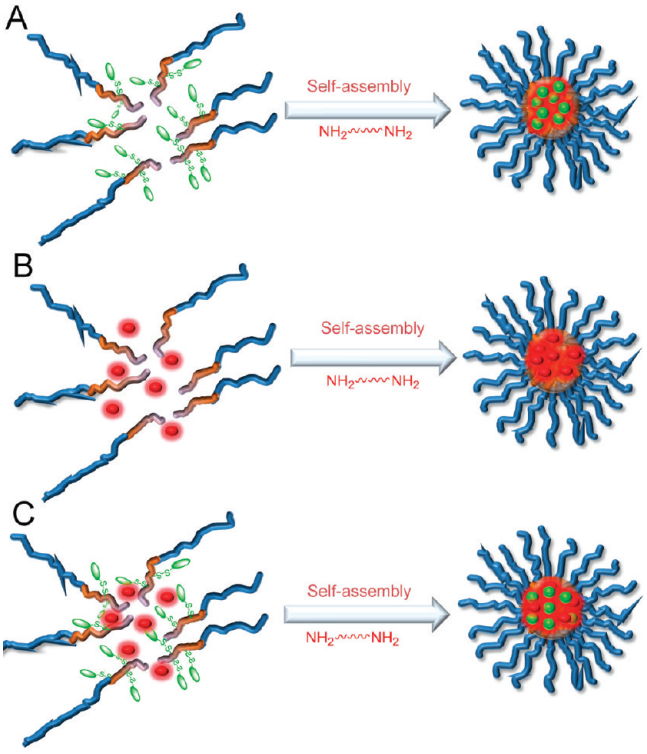

calibration, but it still can gives a qualitative assessment, confirming the presence of cross-linked nanoparticles.

To confirm their pH-sensitive nature, the nanoparticles stabilized with cross-linker **2** were treated with acid (pH = 5.0) for 24 h. The formation of free block copolymer unimers, indicating the breakdown of the core network and nanoparticles disassembly, was confirmed via GPC with a significant shift in the chromatogram from high molecular weight to low molecular weight (from 125 000 to 22 000 g mol^{-1}) (Figure 3).

DLS analysis was also used to determine the hydrodynamic size of the prepared nanoparticles in solution (Figure 4 and Figure S11 in the Supporting Information show volume and intensity size distributions). The sizes of un-cross-linked nanoparticles (ca. 20 nm) in water were found to be slightly smaller than that of cross-linked nanoparticles (ca. 15 nm) attributed to a contraction of the core during the reaction of cross-linking. After treatment with acid (pH 5.0), the sizes of the cross-linked nanoparticles in water were similar to the un-cross-linked nanoparticles as the micellar structure was maintained in water due to the amphiphilic nature of the resulting block copolymer at this concentration (Figure S12 in the Supporting Information). In contrast, when transferred to DMAC (a good solvent for both blocks), the formation of free block copolymers (unimers) is clearly seen by the significant decrease of the cross-linked nanoparticle sizes (from 20 to 6 nm), confirming the dissociation of the network in the core and the formation of unimer.

Encapsulation and Triggered Release of Guest Molecules. An ideal drug delivery system should exhibit the following properties: ability to (i) encapsulate the drug for transit in the bloodstream; (ii) prolong biocirculation, and (iii) stimulated

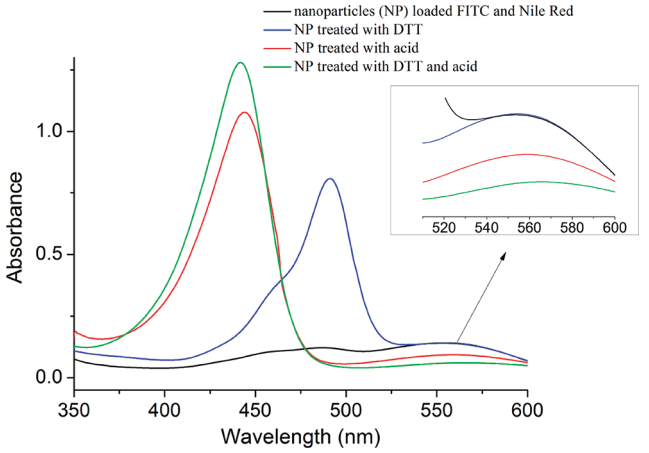

Figure 5. Release of guest molecules from cross-linked nanoparticles after treatment with different triggers.

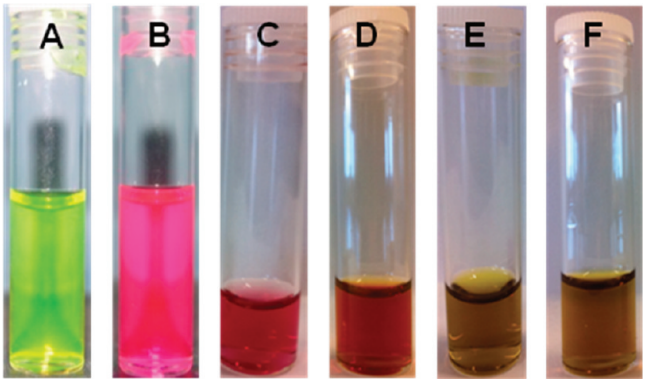

Figure 6. Color changes of nanoparticle (NP) solutions in acidic and/or reductive environments: A, NP loaded with FITC; B,NP loaded with Nile Red; C, NP loaded with FITC and Nile Red; D, NP loaded with FITC and Nile Red treated with DTT (20 mM); E, NP loaded with FITC and Nile Red at pH = 5.0; F, NP loaded with FITC and Nile Red at pH = 5.0 and with DTT (20 mM).

release of the drug into targeted cells in a controlled manner.[86,87] In consideration of these criteria, we predesigned these nanoparticles to encapsulate model guest molecules by reversible covalent attachment (disulfide linkage) and/or by hydrophobic interactions. In this study, thiol-functionalized fluorescein and Nile Red were used as model drugs. The presence of MTS group in the core of the nanoparticles was exploited to attach thiolated fluorescein through disulfide linkage and the release of methyl sulfonate (sulfinic acid).[75,88] Additionally, the hydrophobic cores of the nanoparticles can serve as a suitable reservoir to accommodate hydrophobic guest molecules through nonspecific hydrophobic interactions. The hydrophilic P(OEG-A) brushlike shells protect the cargo from nonspecific binding of proteins while maintain long blood-circulation times.[87,89]

The loading of hydrophilic thiol-modified fluorescein isothiocyanate (FITC) within the hydrophobic core of the nanoparticles is outlined in Scheme 3A. Thiol-modified FITC and copolymer were codissolved in DMF and stirred overnight to allow that the thiol−MTS exchange reaction occurs. The FITC-modified copolymer was then self-assembled to form a micelle by the slow addition of water. Cross-linker **2** was then added to stabilize the nanoparticles. The nanoparticles were purified by dialysis against water to remove both unreacted water-soluble thiolated FITC and cross-linker. The nanoparticle solution remained green after exhaustive dialysis against water (5 days), indicating successful modification (Figure 6A). A control experiment was carried out using non-thiolated FITC where after dialysis the nanoparticle solution was colorless, indicating the absence of nonspecific interaction between the dye and the nanoparticles (UV−vis spectra are reported in Figure S13 of the Supporting Information). FITC-functionalized cross-linked nanoparticles were analyzed by DLS and by TEM. DLS results confirmed the presence of nanoparticles with average sizes slightly larger than the unloaded nanoparticles (25 nm compared to 15 nm in water, Figure S14A in the Supporting Information). The slight increase of the size can be attributed to the attachment of FITC (hydrophilic compound) in the copolymer, resulting in a change of hydrophibicity of the core. The spherical morphology of the nanoparticles was confirmed by TEM (Figure S14B in the Supporting Information). Finally, UV−vis spectroscopy measurements yielded an absorbance peak at 484 nm attributed to the FITC moiety conjugated to the nanoparticles (Figure S14 in the Supporting Information). The yield of the conjugation was calculated via the following equation: FITC yield (%) = $(\lambda^{FITC}/\varepsilon^{FITC})/[VBC]$, with λ^{FITC}, ε^{FITC}, and [VBC] correspond to absorbance at 484 nm and extension coefficient of FITC and concentration of VBC, respectively. The reaction between thiol-modified FITC and MTS is quantitative (yield = 100%).

After addition of a reducing agent DTT and stirring for 24 h at 37 °C, the sample was dialyzed against water. A decrease of the absorbance of FITC was observed by UV−vis spectroscopy during the dialysis, confirming the release of FITC from the nanoparticles (Figure S15 in the Supporting Information). As a control experiment, nontreated FITC nanoparticles were dialyzed under similar conditions; we did not observe any release of FITC (no change in the UV−vis absorbance was detected; data not shown).

To test the capacity of the nanoparticles to store and release hydrophobic drugs via hydrophobic interactions, we studied the loading of Nile Red, a hydrophobic dye. As Nile Red is inherently insoluble in water, the dye was dissolved in DMF with the block copolymer prior to micellization (Scheme 3B). Water was then added to this solution, forming nanoparticles. The acid degradable amine bearing cross-linker **2** was added for the subsequent stabilization of nanoparticles and for the prevention of fast leakage of the guest molecules.[9] The presence of Nile Red inside the nanoparticles was confirmed by UV−vis spectroscopy and by observation of a pink micellar solution after careful purification via dialysis (Figure 6B and Figure S16 in the Supporting Information). Dye loading did not significantly alter the nanoparticle size as determined by DLS (around 22 nm). The addition of acidic solution (pH = 5) resulted in a loss of pink color and precipitation of released Nile Red dye in water, confirming successful acid hydrolysis of the cross-linker (Figure S17 in the Supporting Information). A slight shift of Nile Red absorption maximum was observed from 540 nm (cross-linked nanoparticle) to 575 nm (un-cross-linked nanoparticles) attributed to the change of hydrophobicity environment due to the degradation of the cross-linker. This observed shift in the absorption maximum is in agreement with previous observations reported in the literature;[90,91] the UV−vis absorbance spectrum of Nile Red is sensitive to the environment.

Scheme 4. Schematic Representation for the Release of Nile Red and FITC via Different Stimulus (Reducing Agent: DTT; Acidic Conditions)

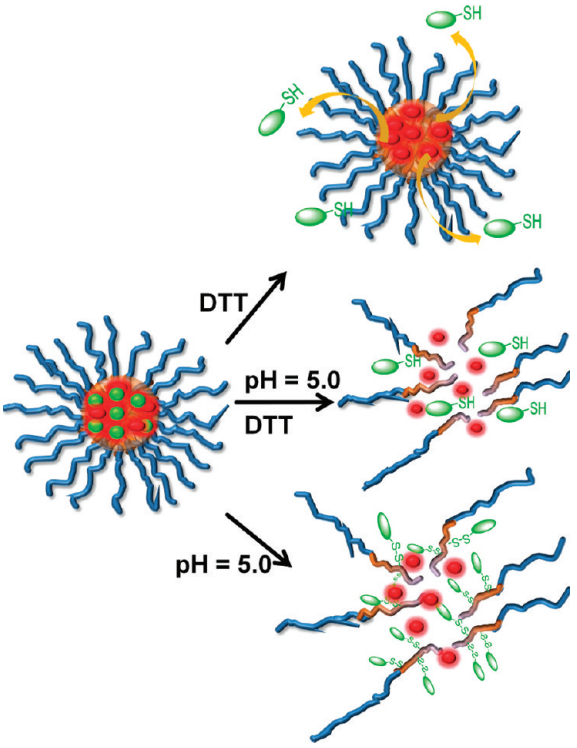

Finally, we simultaneously loaded both dyes using the loading technique described previously (Scheme 3C), and the release of these guest molecules under specific conditions was investigated. Briefly, thiol-modified FITC and the copolymer were dissolved in DMF, and the thiol−MTS exchange reaction was carried out overnight. Nile Red was then added to the solution. Subsequently, water was added very slowly to the DMF solution, followed by the addition of cross-linker **2**. The polymer nanoparticle solution was stirred for several hours and purified by dialysis against water for 2 days. The presence of two dyes was confirmed the presence of two absorption maxima centered at 484 and 565 nm in the UV−vis spectrum (black lines in Figure 5). We note that Nile Red shows a higher absorption maximum (565 nm) in the nanoparticles containing FITC compared to the nanoparticles without FITC (540 nm). We attribute this shift to the slight difference of hydrophobicity of the core due to the presence of FITC.[90] The average size of nanoparticles loaded with FITC and Nile Red was 33 nm, with a polydispersity around 0.1 as assessed by DLS and by TEM. The cross-linked micelles loaded with these two model dyes show high stability in water with no dissociation and precipitation observed for a prolonged period of time (at least 30 days).

The nanoparticles containing both dyes and the ketal cross-linker were subjected to the addition of reducing agent, DTT (20 mM), leading to the disruption of the disulfide bonds and subsequent release of modified FITC from the cores (blue line) (Scheme 4). Under these conditions, the micelle core stayed intact and the Nile Red remained entrapped in the core. A color change was observed from cardinal red to orange (Figure 6). The absorption intensity of FITC in the aqueous reservoir dramatically increased, while the absorption intensity of Nile Red

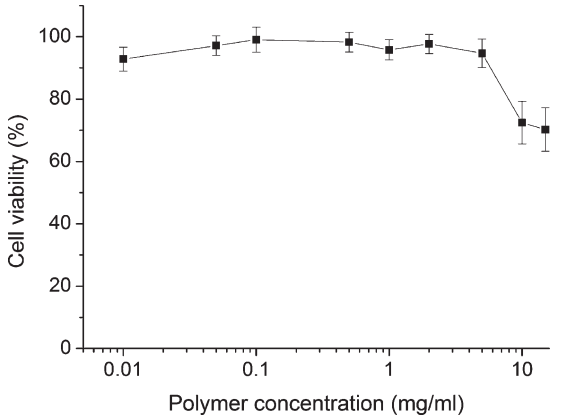

Figure 7. Cytotoxicity data for un-cross-linked P(OEG-A)-*b*-P(VBC-*co*-PFP-A) block copolymers (NIH-3T3 cell viability).

remained unchanged, indicating that the green dye was transferred from the core of nanoparticles to the external aqueous environment, while the hydrophobic guest molecules (Nile Red) remained trapped inside. Prior to DTT treatment, the low UV−vis absorbance signal from FITC (black line) is attributed to the hydrophobic environment of the core due to the presence of Nile Red. The FITC absorbance intensity is affected by the hydrophobicity of its environment.[92,93] The sample was dialyzed against water (as FITC is water-soluble), and the release of green dye from the dialysis bag into the aqueous reservoir was observed. UV−vis spectroscopy confirms that the FITC was quantitatively and selectively released from the nanoparticles by DTT treatment. The nanoparticles contained only Nile Red at the initial concentration.

The release of Nile Red was then stimulated by acid treatment (pH = 5.0, for 24 h) (Scheme 4). The cross-linked nanoparticles degraded under mildly acidic conditions as previously confirmed by GPC data. The release of Nile Red was quantified by the decrease in the UV absorption at 565 nm (red line), although we did not observe 100% efficiency of release, with around 25% remaining trapped within the hydrophobic cores. Simultaneously, the UV absorption peak of modified FITC was shifted to shorter wavelength (blue shift) with increased intensity in the acidic environment as reported in the literature.[94]

Subsequently, the simultaneous release of both guest molecules in a reductive and acidic environment was investigated using DTT (20 mM) and acid (pH = 5.0) treatment (Scheme 4). UV−vis spectroscopy data confirmed a decrease in Nile Red absorption at 570 nm with concomitant precipitation in water (80% of Nile Red release). The increase in the FITC absorption at 484 nm is consistent with a change in configuration of FITC in acid conditions. The sample was dialyzed against water and no FITC release was observed.

In summary, these results reveal that the guest molecules can be coloaded into these polymeric nanoparticles, and their release can be either be specifically or simultaneously stimulated by acidic (pH around 5.5) and/or reductive environments.

Cell Uptake and *in Vitro* Cytotoxicity of the Nanoparticles. The cytotoxicity and cell uptake of these nanoparticles were assessed in a normal cell line (NIH-3T3 cells, fibroblast cell). This cell line is well-known and widely used for cytotoxicity studies.[95,96]

Cytotoxicity Data. The result of the cytotoxicity studies to NIH-3T3 cells are given in Figure 7; the un-cross-linked nanoparticles were found to be nontoxic for NIH-3T3 cells (cell viability above 90%) in the concentration range 0.01−8

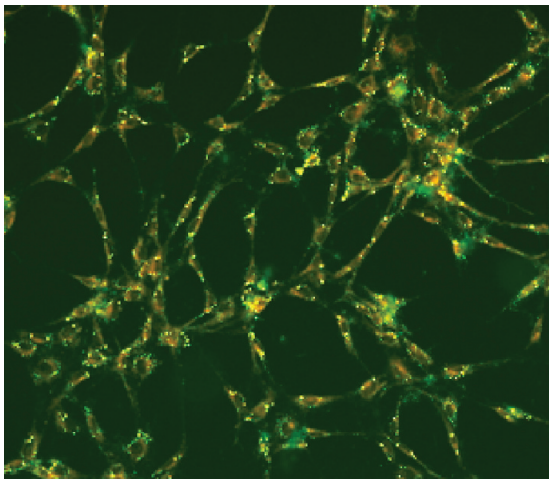

Figure 8. Cellular uptake of nanoparticles by fluorescence microscopy of NIH-3T3 cells treated with cross-linked nanoparticles loaded with FITC and Nile Red.

mg mL^{-1}. Above 8 mg/mL^{-1}, the nanoparticles start exhibiting slight cytotoxic behavior. However, this concentration is very high for clinical applications. In addition, these results reveal that the trithiocarbonate end group is not toxic under these conditions, which is in agreement with previous studies.[95,96]

Cell Uptake Measurements. The cell uptake of the FITC modified nanoparticles can be easily assessed by both fluorescence microscopy (Figure S18 in the Supporting Information) and flow cytometry (Figure S19 in the Supporting Information).

Fluorescence concentration (FC) representing the normalization of cell size or volume with fluorescence intensity was measured for nontreated cells (as a control) and treated cells via flow cytometry. As shown in Figure S19, nanoparticles were efficiently taken up by the cells as indicated by a significant shift in fluorescence concentration between the untreated NIH-3T3 cells and the treated cells. Under these conditions the cell uptake of cross-linked nanoparticles was found to be 10% higher than that of un-cross-linked nanoparticles by comparing the FC values. Side light scattered from the cells was collected and showed no difference in the granularity of cells (with or without treatment with nanoparticles). The slightly higher cell uptake of cross-linked nanoparticles has also been reported by others.[97] This observation is explained by the possible depletion of the number of unstable un-cross-linked nanoparticles, forming unimers, in the culture medium, while the stabilized nanoparticles remain intact and can be taken up by the endocytosis process.

The cell uptake of un-cross-linked and cross-linked nanoparticles was also monitored using fluorescence microscopy after the cells were incubated with nanoparticles for 48 h at 37 °C (Figure S18 in the Supporting Information). The fluorescence intensity is higher for the cells treated with cross-linked nanoparticles, confirming higher cell uptake compared to un-cross-linked nanoparticles. The cellular uptake of cross-linked nanoparticles loaded with FITC and Nile Red can be clearly seen in Figure 8. The nanoparticles taken up by cells became yellow, characteristic of an overlap of green and red emissions, excited by a blue light.

CONCLUSIONS

Orthogonally multifunctional and stable nanoparticles have been synthesized via the self-assembly of intelligently predesigned diblock copolymers. The resultant polymer nanoparticles were used to encapsulate different payloads, hydrophilic and hydrophobic, using specific (degradable bonds) and nonspecific (hydrophobic) interactions. Cell studies (using the NIH-3T3 cell line) indicated that the nanoparticles were readily taken up by these cells and were importantly nontoxic. By introducing dyes as model drugs, we have demonstrated that covalently and noncovalently loaded guest molecules could be released in response to biologically relevant environmental triggers (redox and acid responsive). Future work will focus on the simultaneous loading and stimulated release of both siRNA and chemotherapeutic agents.

ASSOCIATED CONTENT

Supporting Information. Experimental details (PFP-A conversion, PFP-A composition), characterization method, ^{1}H NMR spectra of PFP-A, compounds **1** and **2**, P(OEG-A) homopolymer, UV−vis spectra, GPC data, and TEM micrographs. This material is available free of charge via the Internet at http://pubs.acs.org.

AUTHOR INFORMATION

Corresponding Author

*E-mail: t.davis@unsw.edu.au (T.P.D.); cboyer@unsw.edu.au (C.B.).

ACKNOWLEDGMENT

The authors acknowledge A/Prof. Grainne Moran for her help in the discussion of the absorption of the dyes, Dr. Cindy Gunawan for helping with flow cytometry, and the Australian Reseach Council (ARC) for Discovery grant funding (DP1-092640 and DP110104251). In addition, we acknowledge significant research fellowship from ARC funding to T.P.D. (Federation Fellowship) and C.B. (Australian Postdoctoral Fellowship).

REFERENCES

(1) Soppimath, K. S.; Aminabhavi, T. M.; Kulkarni, A. R.; Rudzinski, W. E. *J. Controlled Release* **2001**, *70*, 1–20.
(2) Kumari, A.; Yadav, S. K.; Yadav, S. C. *Colloids Surf., B* **2010**, *75*, 1–18.
(3) Lee, Y.; Ishii, T.; Cabral, H.; Kim, H. J.; Seo, J.-H.; Nishiyama, N.; Oshima, H.; Osada, K.; Kataoka, K. *Angew. Chem., Int. Ed.* **2009**, *48*, 5309–12.
(4) Lee, Y.; Ishii, T.; Kim, H. J.; Nishiyama, N.; Hayakawa, Y.; Itaka, K.; Kataoka, K. *Angew. Chem., Int. Ed.* **2010**, *49*, 2552–55.
(5) Murakami, M.; Cabral, H.; Matsumoto, Y.; Wu, S.; Kano, M. R.; Yamori, T.; Nishiyama, N.; Kataoka, K. *Sci. Transl. Med.* **2011**, *3*, 64ra2.
(6) Greish, K. *J. Drug Targeting* **2007**, *15*, 457–64.
(7) Farokhzad, O. C.; Langer, R. *ACS Nano* **2009**, *3*, 16–20.
(8) Ryu, J.-H.; Jiwpanich, S.; Chacko, R.; Bickerton, S.; Thayumanavan, S. *J. Am. Chem. Soc.* **2010**, *132*, 8246–47.
(9) Ryu, J. H.; Chacko, R. T.; Jiwpanich, S.; Bickerton, S.; Babu, R. P.; Thayumanavan, S. *J. Am. Chem. Soc.* **2010**, *132*, 17227–35.
(10) Jiwpanich, S.; Ryu, J.-H.; Bickerton, S.; Thayumanavan, S. *J. Am. Chem. Soc.* **2010**, *132*, 10683–85.
(11) Kim, Y.; Pourgholami, M. H.; Morris, D. L.; Stenzel, M. H. *Macromol. Bioscience* **2011**, *11*, 219–33.
(12) Syrett, J. A.; Haddleton, D. M.; Whittaker, M. R.; Davis, T. P.; Boyer, C. *Chem. Commun.* **2011**, *47*, 1449–51.
(13) Kataoka, K.; Harada, A.; Nagasaki, Y. *Adv. Drug Delivery Rev.* **2001**, *47*, 113–31.
(14) Mezei, M.; Gulasekharam, V. *Life Sci.* **1980**, *26*, 1473–77.

(15) Sharma, A.; Sharma, U. S. *Int. J. Pharm.* **1997**, *154*, 123–40.
(16) Jia, Z.; Liu, J.; Boyer, C.; Davis, T. P.; Bulmus, V. *Biomacromolecules* **2009**, *10*, 3253–58.
(17) Matyjaszewski, K.; Tsarevsky, N. V. *Nature Chem.* **2009**, *1*, 276–88.
(18) Li, W.; Matyjaszewski, K. *Macromol. Rapid Commun.* **2011**, *32*, 74–81.
(19) Gao, H.; Matyjaszewski, K. *Prog. Polym. Sci.* **2009**, *34*, 317–50.
(20) Deng, G.; Cao, M.; Huang, J.; He, L.; Chen, Y. *Polymer* **2005**, *46*, 5698–701.
(21) Ouchi, M.; Terashima, T.; Sawamoto, M. *Acc. Chem. Res.* **2008**, *41*, 1120–32.
(22) Blencowe, A.; Tan, J. F.; Goh, T. K.; Qiao, G. G. *Polymer* **2009**, *50*, 5–32.
(23) Hou, S.; Chaikof, E. L.; Taton, D.; Gnanou, Y. *Macromolecules* **2003**, *36*, 3874–81.
(24) Boyer, C.; Stenzel, M. H.; Davis, T. P. *J. Polym. Sci., Part A: Polym. Chem.* **2011**, *49*, 551–95.
(25) Moad, G. *Aust. J. Chem.* **2006**, *59*, 661–62.
(26) Chaffey-Millar, H.; Stenzel, M. H.; Davis, T. P.; Coote, M. L.; Barner-Kowollik, C. *Macromolecules* **2006**, *39*, 6406–19.
(27) Stenzel, M. H.; Davis, T. P. *J. Polym. Sci., Part A: Polym. Chem.* **2002**, *40*, 4498–512.
(28) Moad, G.; Chong, Y. K.; Postma, A.; Rizzardo, E.; Thang, S. H. *Polymer* **2005**, *46*, 8458–68.
(29) Ranganathan, K.; Deng, R.; Kainthan, R. K.; Wu, C.; Brooks, D. E.; Kizhakkedathu, J. N. *Macromolecules* **2008**, *41*, 4226–34.
(30) Taton, D.; Baussard, J.-F.; Dupayage, L.; Gnanou, Y.; Destarac, M.; Mignaud, C.; Pitois, C. In *Controlled/Living Radical Polymerization*; American Chemical Society: Washington, DC, 2006; Vol. 944, pp 578−94.
(31) Duréault, A.; Taton, D.; Destarac, M.; Leising, F.; Gnanou, Y. *Macromolecules* **2004**, *37*, 5513–19.
(32) Boyer, C.; Bulmus, V.; Davis, T. P.; Ladmiral, V.; Liu, J.; Perrier, S. b. *Chem. Rev.* **2009**, *109*, 5402–36.
(33) Moad, G.; Rizzardo, E.; Thang, S. H. *Acc. Chem. Res.* **2008**, *41*, 1133–42.
(34) Iha, R. K.; Wooley, K. L.; Nyström, A. M.; Burke, D. J.; Kade, M. J.; Hawker, C. J. *Chem. Rev.* **2009**, *109*, 5620–86.
(35) Roth, P. J.; Boyer, C.; Lowe, A. B.; Davis, T. P. *Macromol. Rapid Commun.* **2011**, *32*, 1123–1143.
(36) O'Reilly, R. K.; Hawker, C. J.; Wooley, K. L. *Chem. Soc. Rev.* **2006**, *35*, 1068–83.
(37) Sumerlin, B. S.; Vogt, A. P. *Macromolecules* **2009**, *43*, 1–13.
(38) Beck, J. B.; Killops, K. L.; Kang, T.; Sivanandan, K.; Bayles, A.; Mackay, M. E.; Wooley, K. L.; Hawker, C. J. *Macromolecules* **2009**, *42*, 5629–35.
(39) Joralemon, M. J.; O'Reilly, R. K.; Hawker, C. J.; Wooley, K. L. *J. Am. Chem. Soc.* **2005**, *127*, 16892–99.
(40) O'Reilly, R. K.; Joralemon, M. J.; Hawker, C. J.; Wooley, K. L. *Chem.—Eur. J.* **2006**, *12*, 6776–86.
(41) O'Reilly, R. K.; Joralemon, M. J.; Hawker, C. J.; Wooley, K. L. *J. Polym. Sci., Part A: Polym. Chem.* **2006**, *44*, 5203–17.
(42) O'Reilly, R. K.; Joralemon, M. J.; Hawker, C. J.; Wooley, K. L. *New J. Chem.* **2007**, *31*, 718–24.
(43) O'Reilly, R. K.; Joralemon, M. J.; Wooley, K. L.; Hawker, C. J. *Chem. Mater.* **2005**, *17*, 5976–88.
(44) Sun, G.; Xu, J.; Hagooly, A.; Rossin, R.; Li, Z.; Moore, D. A.; Hawker, C. J.; Welch, M. J.; Wooley, K. L. *Adv. Mater.* **2007**, *19*, 3157–62.
(45) Takae, S.; Miyata, K.; Oba, M.; Ishii, T.; Nishiyama, N.; Itaka, K.; Yamasaki, Y.; Koyama, H.; Kataoka, K. *J. Am. Chem. Soc.* **2008**, *130*, 6001–9.
(46) Lee, Y.; Miyata, K.; Oba, M.; Ishii, T.; Fukushima, S.; Han, M.; Koyama, H.; Nishiyama, N.; Kataoka, K. *Angew. Chem., Int. Ed.* **2008**, *47*, 5163–66.
(47) Zhang, H.; Wang, G.; Yang, H. *Exp. Opinion Drug Delivery* **2011**, *8*, 171–90.
(48) Singh, A.; Dilnawaz, F.; Mewar, S.; Sharma, U.; Jagannathan, N. R.; Sahoo, S. K. *ACS Appl. Mater. Interfaces* **2011**, *3*, 842–56.
(49) Mok, H.; Veiseh, O.; Fang, C.; Kievit, F. M.; Wang, F. Y.; Park, J. O.; Zhang, M. *Mol. Pharmaceutics* **2010**, *7*, 1930–39.
(50) Patil, Y. B.; Swaminathan, S. K.; Sadhukha, T.; Ma, L.; Panyam, J. *Biomaterials* **2010**, *31*, 358–65.
(51) Qiu, L. Y.; Bae, Y. H. *Biomaterials* **2007**, *28*, 4132–42.
(52) Zhu, W.; Li, Y.; Liu, L.; Zhang, W.; Chen, Y.; Xi, F. *J. Biomed. Mater. Res., Part A* **2011**, *96A*, 330–40.
(53) Kolishetti, N.; Dhar, S.; Valencia, P. M.; Lin, L. Q.; Karnik, R.; Lippard, S. J.; Langer, R.; Farokhzad, O. C. *Proc. Natl. Acad. Sci. U. S. A.* **2010**, *107*, 17939–44.
(54) Wang, Z.; Ho, P. C. *Biomaterials* **2010**, *31*, 7115–23.
(55) Patil, Y.; Sadhukha, T.; Ma, L.; Panyam, J. *J. Controlled Release* **2009**, *136*, 21–29.
(56) Wang, Z.; Chui, W.-K.; Ho, P. *Pharm. Res.* **2011**, *28*, 585–96.
(57) Li, Z.; Kesselman, E.; Talmon, Y.; Hillmyer, M. A.; Lodge, T. P. *Science* **2004**, *306*, 98–101.
(58) Saito, N.; Liu, C.; Lodge, T. P.; Hillmyer, M. A. *ACS Nano* **2010**, *4*, 1907–12.
(59) Li, Z.; Hillmyer, M. A.; Lodge, T. P. *Langmuir* **2006**, *22*, 9409–17.
(60) Jiang, T.; Wang, L.; Lin, S.; Lin, J.; Li, Y. *Langmuir* **2011**, *27*, 6440–48.
(61) Delcea, M.; Yashchenok, A.; Videnova, K.; Kreft, O.; Möhwald, H.; Skirtach, A. G. *Macromol. Biosci.* **2010**, *10*, 465–74.
(62) Lutz, J.-F.; Laschewsky, A. *Macromol. Chem. Phys.* **2005**, *206*, 813–17.
(63) Sankaranarayanan, J.; Mahmoud, E. A.; Kim, G.; Morachis, J. M.; Almutairi, A. *ACS Nano* **2010**, *4*, 5930–36.
(64) Theato, P. *J. Polym. Sci., Part A: Polym. Chem.* **2008**, *46*, 6677–87.
(65) Gauthier, M. A.; Gibson, M. I.; Klok, H.-A. *Angew. Chem., Int. Ed.* **2009**, *48*, 48–58.
(66) Barz, M.; Tarantola, M.; Fischer, K.; Schmidt, M.; Luxenhofer, R.; Janshoff, A.; Theato, P.; Zentel, R. *Biomacromolecules* **2008**, *9*, 3114–18.
(67) Hwang, J.; Li, R. C.; Maynard, H. D. *J. Controlled Release* **2007**, *122*, 279–86.
(68) Nilles, K.; Theato, P. *J. Polym. Sci., Part A: Polym. Chem.* **2010**, *48*, 3683–92.
(69) Boyer, C.; Davis, T. P. *Chem. Commun.* **2009**, 6029–31.
(70) Singha, N. K.; Gibson, M. I.; Koiry, B. P.; Danial, M.; Klok, H.-A. *Biomacromolecules* **2011**, *12* (8), 2908–2913.
(71) Quinn, J. F.; Chaplin, R. P.; Davis, T. P. *J. Polym. Sci., Part A: Polym. Chem.* **2002**, *40*, 2956–66.
(72) Boyer, C.; Bulmus, V.; Davis, T. P. *Macromol. Rapid Commun.* **2009**, *30*, 493–97. Boyer, C.; Granville, A.; Davis, T. P.; Bulmus, V. *J. Polym. Sci., Part A: Polym. Chem.* **2009**, *47*, 3773–3794.
(73) Paramonov, S. E.; Bachelder, E. M.; Beaudette, T. T.; Standley, S. M.; Lee, C. C.; Dashe, J.; Fréchet, J. M. J. *Bioconjugate Chem.* **2008**, *19*, 911–19.
(74) Jain, R.; Standley, S. M.; Frechet, J. M. J. *Macromolecules* **2007**, *40*, 452–57.
(75) Boyer, C.; Soeriyadi, A. H.; Roth, P. J.; Whittaker, M. R.; Davis, T. P. *Chem. Commun.* **2011**, *47*, 1318–20.
(76) Zhang, L. F.; Eisenberg, A. *Science* **1995**, *268*, 1728–31.
(77) Zhang, L. F.; Eisenberg, A. *Polym. Adv. Technol.* **1998**, *9*, 677–99.
(78) Zhang, L. F.; Eisenberg, A. *J. Polym. Sci., Part B: Phys. Chem.* **1999**, *37*, 1469–84.
(79) Zhang, L. F.; Eisenberg, A. *Macromolecules* **1999**, *32*, 2239–49.
(80) Soo, P. L.; Eisenberg, A. *J. Polym. Sci., Part B: Polym. Phys.* **2004**, *42*, 923–38.
(81) Hamley, I. *Block Copolymers in Solution: Fundamentals and Applications*; John Wiley and Sons, Ltd.: New York, 2005.
(82) Duong, H. T. T.; Nguyen, T. L. U.; Stenzel, M. *Polym. Chem.* **2010**, *1*, 171.

(83) Croy, S. R.; Kwon, G. S. *Curr. Pharm. Des.* **2006**, *12*, 4669–84.
(84) Poland, D. C.; Scheraga, H. A. *J. Phys. Chem.* **1965**, *69*, 2431–42.
(85) Ferreira, J.; Syrett, J.; Whittaker, M.; Haddleton, D.; Davis, T. P.; Boyer, C. *Polym. Chem.* **2011**, *2*, 1671–1677.
(86) Scholz, C.; Iijima, M.; Nagasaki, Y.; Kataoka, K. *Polym. Adv. Technol.* **1998**, *9*, 768–76.
(87) Lu, J.; Owen, S. C.; Shoichet, M. S. *Macromolecules* **2011**, *44* (15), 6002–6008.
(88) Roth, P. J.; Kessler, D.; Zentel, R.; Theato, P. *J. Polym. Sci., Part A: Polym. Chem.* **2009**, *47*, 3118–30.
(89) Lee, H.; Lee, E.; Kim, D. K.; Jang, N. K.; Jeong, Y. Y.; Jon, S. *J. Am. Chem. Soc.* **2006**, *128*, 7383–89.
(90) Dutta, A. K.; Kamada, K.; Ohta, K. *J. Photochem. Photobiol. A: Chem.* **1996**, *93*, 57–64.
(91) Greenspan, P.; Fowler, S. D. *J. Lipid Res.* **1985**, *26*, 781–9.
(92) Biswas, S.; Bhattacharya, S. C.; Sen, P. K.; Moulik, S. P. *J. Photochem. Photobiol. A: Chem.* **1999**, *123*, 121–28.
(93) Song, A.; Zhang, J.; Zhang, M.; Shen, T.; Tang, J. A. *Colloids Surf., A* **2000**, *167*, 253–62.
(94) Sjöback, R.; Nygren, J.; Kubista, M. *Spectrochim. Acta, Part A* **1995**, *51*, L7–L21.
(95) Chang, C.-W.; Bays, E.; Tao, L.; Alconcel, S. N. S.; Maynard, H. D. *Chem. Commun.* **2009**, 3580–82.
(96) Pissuwan, D.; Boyer, C.; Gunasekaran, K.; Davis, T. P.; Bulmus, V. *Biomacromolecules* **2010**, *11*, 412–20.
(97) Benaglia, M.; Alberti, A.; Spisni, E.; Papi, A.; Treossi, E.; Palermo, V. *J. Mater. Chem.* **2011**, *21*, 2555–62.